



ROBOT-ASSISTED THERAPY: DESIGN, CONTROL AND OPTIMIZATION

Haifa Mehdi¹, Olfa Boubaker²

National Institute of Applied Sciences and Technology
Centre Urbain Nord BP 676, 1080 Tunis Cedex, Tunisia

¹ haifa.mehdi@gmail.com, ² olfa.boubaker@insat.rnu.tn

Submitted: Aug. 16, 2012

Accepted: Oct. 15, 2012

Published: Dec. 1, 2012

Abstract- To improve the human arm function of disable patients after stroke, we propose in this paper a new design of a robot-assisted therapy. The robotic device must be attached to a human arm and mimics the motion of the shoulder, elbow and wrist joints. The functional training of the stroked upper limb is covered in motion and force via a safe compliant motion. The controller parameters are optimized by the therapist based on the human morphology parameters via an intelligent Control Interface where a Therapist-Patient Interface including the training mode configuration and the displaying the training data must motivate the patients during the assessment treatment progress.

Index terms: Robot-assisted therapy, Impedance control, Safe control, Nonlinear optimization, Human Machine Interface.

I. INTRODUCTION

The concept of robotics assisted therapy is one of the most important issues in social robotic research. It was introduced in the 60s [1] and since various robotic devices are proposed to help stroke patients and physiotherapists during the rehabilitation training. Two categories of rehabilitation robots exist: devices designed for upper limbs assisting [2, 3] and devices designed for lower limbs assisting [4, 5]. Many current research works have also proved the interest of robot-assisted therapy to help dependent people with disabilities [6, 7].

For upper limbs assessment, several elaborated robotic devices exist such as the MIT-MANUS robotic device of Massachusetts Institute of Technology [8], the MIME robot of the Stanford University [9] and the RUPERT robotic device of the Arizona State University [10]. Robot assisted therapy systems require three elements: robot hardware, computer system and algorithms [11]. However, the design of the control system remains one of the main difficulties especially when intending to realize predefined complex movements and recovering at the same time motion and force human capabilities [12]. Furthermore, unlike industrial robots, rehabilitation-aided robots must be configured not only for stable motion but also for safe compliant motion in contact with humans [12, 13, 14, 15, 16]. The impedance control strategy initially proposed by Hogan [17] seems to be the most appropriate approach for such task. In this framework, we have recently proposed an improved impedance controller for which the parameters can be designed via two cases. Only one case was discussed in [12] for which the impedance transfer function has a first order model and the controller parameters were optimized via a nonlinear approach.

In this paper we propose a new design of robot assisted therapy actuated by a safe control strategy. We discuss the nonlinear optimization of the controller parameters via the improved impedance controller for the second case where the impedance transfer function has a second order model. Finally, we propose a human machine interface to help the therapist to design the control law and to motivate the patient during the rehabilitation assessment. The contribution in this paper is complementary to our previous works presented for the design of position/force controller laws via Lyapunov approaches [12, 18, 19, 20].

II. THE ROBOT-ASSISTED THERAPY

As shown by Fig.1, the rehabilitation platform is composed by a support system, a linkage system and a 3DOF robotic arm. The support device is designed such it can support the weight of the linkage system and the robotic arm. The linkage system allows the therapist to adjust distances between axes and customize the rehabilitation device for different users based on morphological parameters. The robotic arm (see Fig.2) allows the human upper limb to be attached via two supports to have upper limb joints lined with the robot joints in order to control them independently.

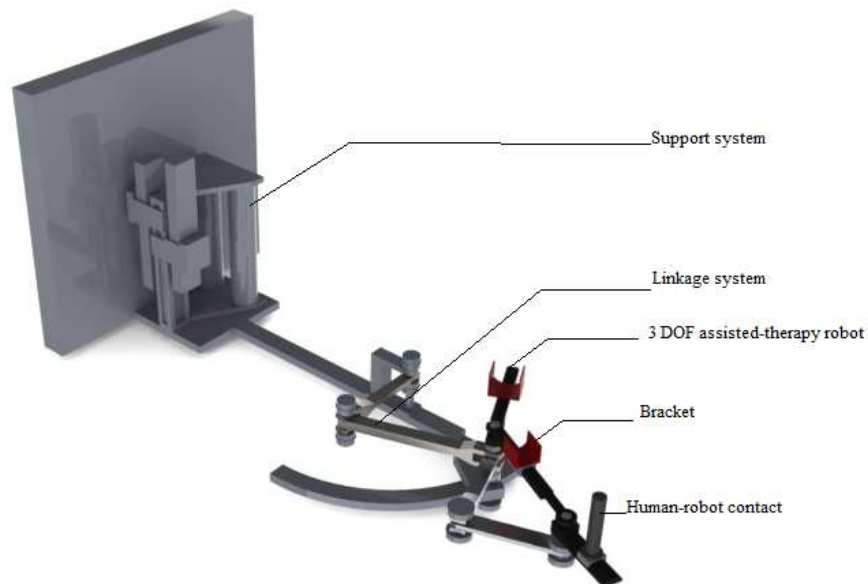


Fig.1. Rehabilitation platform

The kinematic model of the robotic system is described by:

$$\begin{cases} x = L_1 \cos \theta_1 + L_2 \cos \theta_2 + L_3 \cos \theta_3 \\ y = L_1 \sin \theta_1 + L_2 \sin \theta_2 + L_3 \sin \theta_3 \end{cases} \quad (1)$$

The differential kinematic model is defined by:

$$\dot{X} = J(\theta)\dot{\theta} \quad (2)$$

where:

$$J(\theta) = \begin{bmatrix} -L_1 \sin \theta_1 & -L_2 \sin \theta_2 & -L_3 \sin \theta_3 \\ L_1 \cos \theta_1 & L_2 \cos \theta_2 & L_3 \cos \theta_3 \end{bmatrix}$$

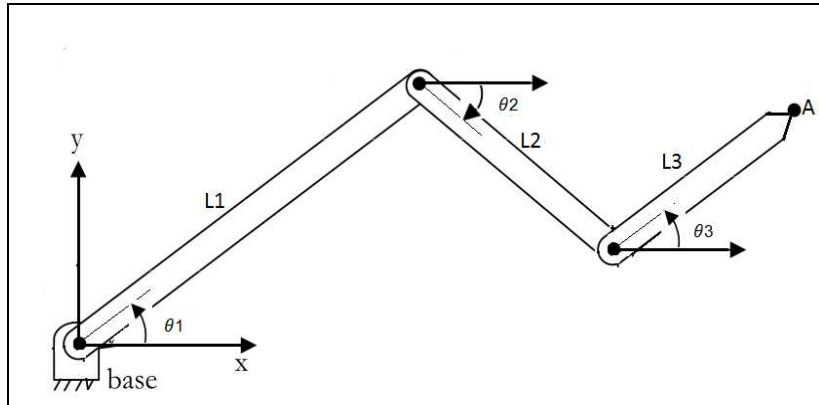


Fig.2. 3DOF robot-aided therapy

and the dynamic model is described by:

$$M(\theta)\ddot{\theta} + H(\theta, \dot{\theta}) + G(\theta) = U - J(\theta)^T F \quad (3)$$

where

$$M(\theta) = \begin{bmatrix} I_1 + m_1 k_1^2 + m_2 L_1^2 + m_3 L_1^2 & (m_2 L_1 k_2 + m_3 L_1 L_2) \cos(\theta_1 - \theta_2) & m_3 L_1 k_2 \cos(\theta_1 - \theta_3) \\ (m_2 L_1 k_2 + m_3 L_1 L_2) \cos(\theta_1 - \theta_2) & I_2 + m_2 k_2^2 + m_3 L_2^2 & m_3 L_2 k_3 \cos(\theta_2 - \theta_3) \\ m_3 L_1 k_2 \cos(\theta_1 - \theta_3) & m_3 L_2 k_3 \cos(\theta_2 - \theta_3) & I_3 + m_3 k_3^2 \end{bmatrix}$$

$$H(\theta, \dot{\theta}) = \begin{bmatrix} 0 & (m_2 L_1 k_2 + m_3 L_1 L_2) \sin(\theta_1 - \theta_2) & m_3 L_1 k_2 \sin(\theta_1 - \theta_3) \\ -(m_2 L_1 k_2 + m_3 L_1 L_2) \sin(\theta_1 - \theta_2) & 0 & m_3 L_2 k_3 \sin(\theta_2 - \theta_3) \\ -m_3 L_1 k_2 \sin(\theta_1 - \theta_3) & -m_3 L_2 k_3 \sin(\theta_2 - \theta_3) & 0 \end{bmatrix} \begin{bmatrix} \dot{\theta}_1^2 \\ \dot{\theta}_2^2 \\ \dot{\theta}_3^2 \end{bmatrix}$$

$$G(\theta) = g \begin{bmatrix} (m_1 k_1 + m_2 L_1 + m_3 L_1) \cos \theta_1 \\ (m_2 k_2 + m_3 L_2) \cos \theta_2 \\ m_3 k_3 \cos \theta_3 \end{bmatrix}$$

$\theta, \dot{\theta}, \ddot{\theta}$ design the joint position, velocity and acceleration vectors, respectively. U is the generalized joint force vector and F is the vector of compliant contact forces exerted by the user on the robotic system. The parameters m_i, L_i and k_i and I_i ($i = 1, 2, 3$) design mass, length, position of gravity center and inertia parameter of each rigid body of the 3DOF robot.

The physical parameters of the robot-assisted therapy are shown in Table 1 and correspond to a right arm, forearm and hand of a stroked patient having a weight of 70 kg and a height of 1.73 m. they are computed using the famous Winter statistical model and referring to [21].

Table1. Robot-assisted therapy physical parameters

joint i	$M_i(\text{Kg})$	$L_i(\text{m})$	$k_i(\text{m})$	$I_i(\text{Kg m}^{-2})$
1	1.960	0.321	0.140	0.016
2	1.120	0.253	0.109	0.006
3	0.420	0.187	0.095	0.001

III. THE SAFE COMPLIANT CONTROL STRATEGY

The control system of the rehabilitation device is designed in order to authorize corrective forces and torques to the human arm. Desired positions are enforced by the robotic system whereas desired contact forces are inflicted by the patient. Furthermore, safety is perquisite further in the therapy. The controller should then impose to the robotic device to track a complex motion trajectory such as circular ones and realize a desired impedance dynamics between the end-effector position and the contact force (see Fig.3). The desired impedance is defined by:

$$Z_d = \frac{F_d - F}{X_d - X} = K_d + B_d s + M_d s^2 \quad M_d \neq 0 \quad (4)$$

where Z_d , X_d and F_d are desired impedance, desired Cartesian position and desired contact force, respectively. $K_d, B_d, M_d \in R^{2 \times 2}$ are desired stiffness, damping and inertia matrices and s is the Laplace operator. We assume in the following that they are diagonal matrices.

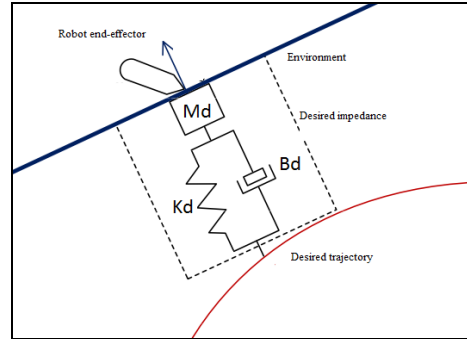


Fig. 3. Desired impedance dynamics between the end-effector position of the robot-assisted therapy and the contact force

Theorem:

For desired matrices $K_d, B_d, M_d \in R^{2 \times 2}$ and if there exist diagonal matrices $K_p, K_v, K_f \in R^{2 \times 2}$ such that the following conditions:

$$\begin{aligned} K_p + (I + K_f)K_d &> 0 \\ K_v + (I + K_f)B_d &> 0 \\ M_d &= 0 \end{aligned} \quad (5)$$

or

$$\begin{aligned} K_p &> 0 \\ K_v &> 0 \\ K_f &= -I \end{aligned} \quad (6)$$

are satisfied, then the robotic system described by the kinematic models (1), the differential kinematic model (2) and the dynamical model (3) is asymptotically stable under the constrained force:

$$F = F_d - K_d (X_d - X) - B_d (\dot{X}_d - \dot{X}) - M_d (\ddot{X}_d - \ddot{X}) \quad (7)$$

and the control law:

$$U = J^T [K_p (X_d - X) + K_v (\dot{X}_d - \dot{X}) + K_f (F_d - F) + F_d] + G \quad (8)$$

Proof: see [12]

IV. COMPLIANT TRAJECTORY

We impose to the robot-aided therapy to follow a circular profile in the Cartesian space. To realize this trajectory, we introduce a sinusoidal signal on each axis of the third joint. Therefore, for a circle radius R , the desired motion of the end-effector of the compliant robot is defined in the Cartesian space by:

$$X_d = \begin{bmatrix} R \cos(\theta_{3,d}(t)) \\ R \sin(\theta_{3,d}(t)) \end{bmatrix} \quad (9)$$

where:

$$\theta_{3,d}(t) = a_0 + a_1 t + a_2 t^2 + a_3 t^3 \quad (10)$$

Taking on account that the motion must begin and end regularly such that for $i = 1, 2, 3$:

$$\begin{aligned} \theta_i(t_0) &= \theta_{i0}; \dot{\theta}_i(t_0) = 0 \\ \theta_i(t_f) &= \theta_{id}; \dot{\theta}_i(t_f) = 0 \end{aligned}$$

where t_0 and t_f design initial and terminal times. Reference joint trajectories are chosen as:

$$\begin{bmatrix} a_0 \\ a_1 \\ a_2 \\ a_3 \end{bmatrix} = \begin{bmatrix} 1 & t_0 & t_0^2 & t_0^3 \\ 1 & t_f & t_f^2 & t_f^3 \\ 0 & 1 & 2t_0 & 3t_0^2 \\ 0 & 1 & 2t_f & 3t_f^2 \end{bmatrix}^{-1} \begin{bmatrix} \theta_{i0} \\ \theta_{id} \\ 0 \\ 0 \end{bmatrix} \quad (11)$$

V. CONTROLLER PARAMETER OPTIMIZATION

Since we have assumed that the inertia matrix is a non null matrix, only the stability conditions (6) will be considered in this paper for solving the optimizing problem. Tuning controller parameters for the stability conditions (5) are previously discussed in [12]. To adjust the parameters of the control law (8) using the stability conditions (5) for the force model (7), the following nonlinear optimization problem is solved for the decision vector $z = \begin{bmatrix} k_p & k_v \end{bmatrix}^T$:

$$\min f(z) \tag{12}$$

subject to the dynamical constraints (1) and (2), the following inequality constraints:

$$\begin{bmatrix} -1 & 0 & -k_d \\ 0 & -1 & -b_d \end{bmatrix} z < \begin{bmatrix} k_d \\ b_d \end{bmatrix} \tag{13}$$

$$100 \leq k_p \leq 700$$

$$30 \leq k_v \leq 400$$

and the following equality constraints:

$$k_f = -1, k_d = 20, b_d = 10, m_d = 0.01 \tag{14}$$

where k_p, k_v, k_f, k_d, b_d and m_d are the diagonal elements of the gain matrices K_p, K_v, K_f, K_d, B_d and M_d , respectively.

$f(z)$ is defined as one of three following functions:

- The Root Squared Error (RSE) of the third joint defined by:

$$RSE = \frac{1}{N} \sum_{i=1}^N \sqrt{e_3^2(i)} \tag{15}$$

- The Mean of the Root Squared Error (MRSE) defined by:

$$MRSE = \frac{1}{N} \sum_{i=1}^N \sqrt{e_1^2(i) + e_2^2(i) + e_3^2(i)} \tag{16}$$

- The Mean of the Absolute Magnitude Error (MAE) defined by:

$$MAE = \frac{1}{N} \sum_{i=1}^N (|e_1(i)| + |e_2(i)| + |e_3(i)|) \tag{17}$$

where $e_1(i), e_2(i)$ and $e_3(i)$ are the trajectory errors of the i th iteration of the first joint, second joint and third joint respectively. N is the iteration number.

The last optimization problem will be solved using the constrained nonlinear optimization method proposed in [22] and solved using the *fmincon* function of the optimization toolbox of MatLab software.

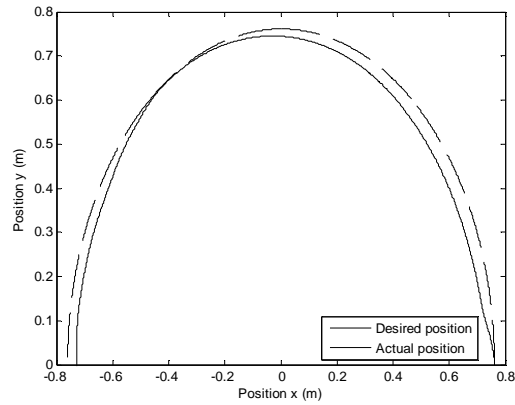
For simulations, the desired contact force is chosen as $F_d = [6 \ 0]^T$ and the initial value of the decision vector is chosen as $z_0 = [500 \ 200]^T$. For the circular motion, we choose a radius of 0.76 m and a movement beginning at $\theta_{i0} = [0 \ 0 \ 0]^T$ and ending at $\theta_{id} = [\pi \ \pi \ \pi]^T$ during 1s ($t_0 = 0$ and $t_f = 1s$).

Best impedance controller parameters and the corresponding objective functions are reported in Table 2.

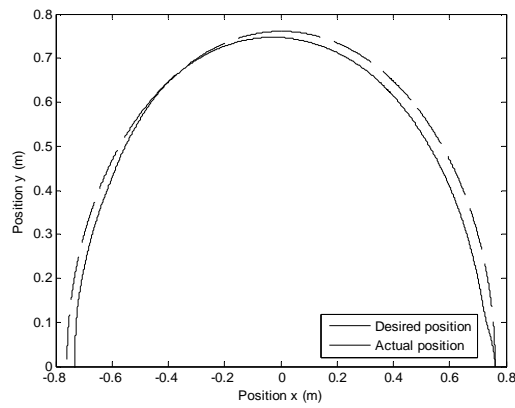
Table 2: Best impedance controller parameters and relating objective functions

Objective function	Objective function value	Decision vector $\begin{bmatrix} k_p & k_v \end{bmatrix}^T$	Optimization time (s)
RSE	0.25	$[570.7 \ 201.4]^T$	1257.5
MRSE	0.22	$[670.8 \ 233.1]^T$	1555.8
MAE	0.18	$[700 \ 350.1]^T$	50.1

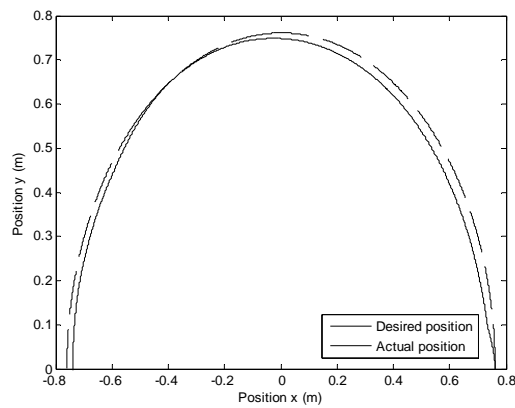
For the decision vectors given in Table 2, simulation results are given in Fig.4 to Fig.6 where the profile of the desired and actual trajectories, contact forces and control laws, are respectively observed. As can be seen, desired Cartesian trajectory is followed for safe force and control laws.



(a)

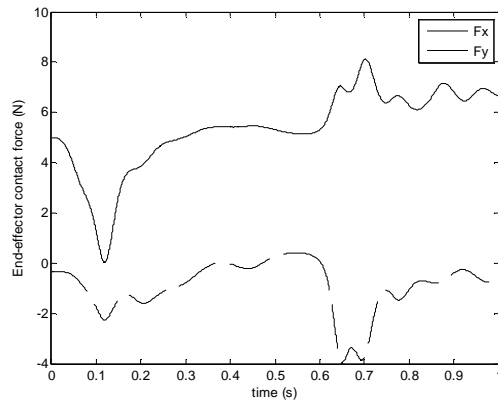


(b)

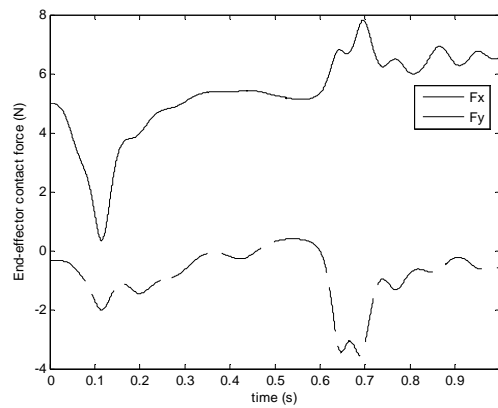


(c)

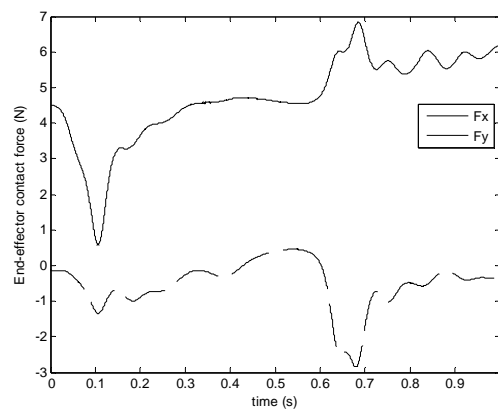
Fig.4. End effector trajectory for controller parameters tuned by: (a) RSE optimization function, (b) MRSE function and (c) MAE function



(a)

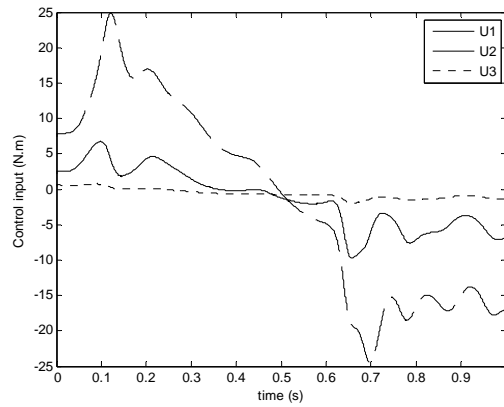


(b)

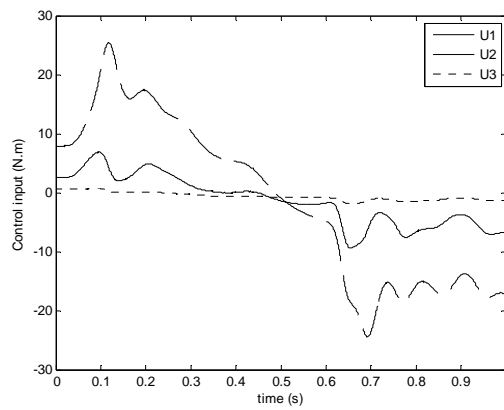


(c)

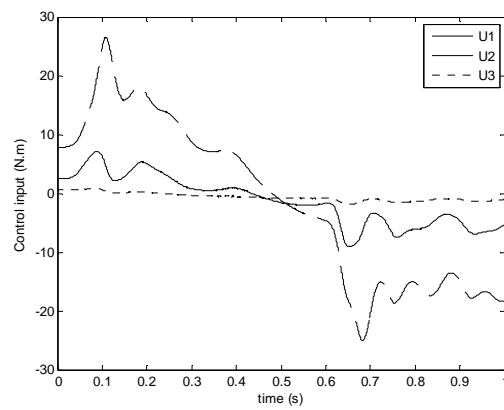
Fig.5. Contact force response for controller parameters tuned by: (a) RSE optimization function, (b) MRSE function and (c) MAE function



(a)



(b)



(c)

Fig.6. Control law profiles for controller parameters tuned by: (a) RSE optimization function, (b) MRSE function and (c) MAE function

VI. SOFTWARE / HARDWARE CONTROL SYSTEM

The implementation of the control system requires two types of interactions: the interaction with the robot and the interaction with the human (therapist and patient in our case). Interaction with the robot necessitates a real time control system of the motor drives which are in the most cases servomotors. For real-time control, two methods are available [11]. One is the use of real-time operating system, see for example [23, 24] and the other is the hybrid control system of a PC and a Micro Control Unit (MCU), see for example control applications presented in [11, 25]. In this paper we use the second approach. We have designed two types of MCU boards, one for acquiring sensor data and a second for writing motor commands. Fig.7 shows, for example, the MCU board designed via Proteus software for reading position, velocity, acceleration and force sensor data using the microcontroller 18F4550 at 48 MHz sampling frequency for one joint. The board communicates with the PC via an USB connector.

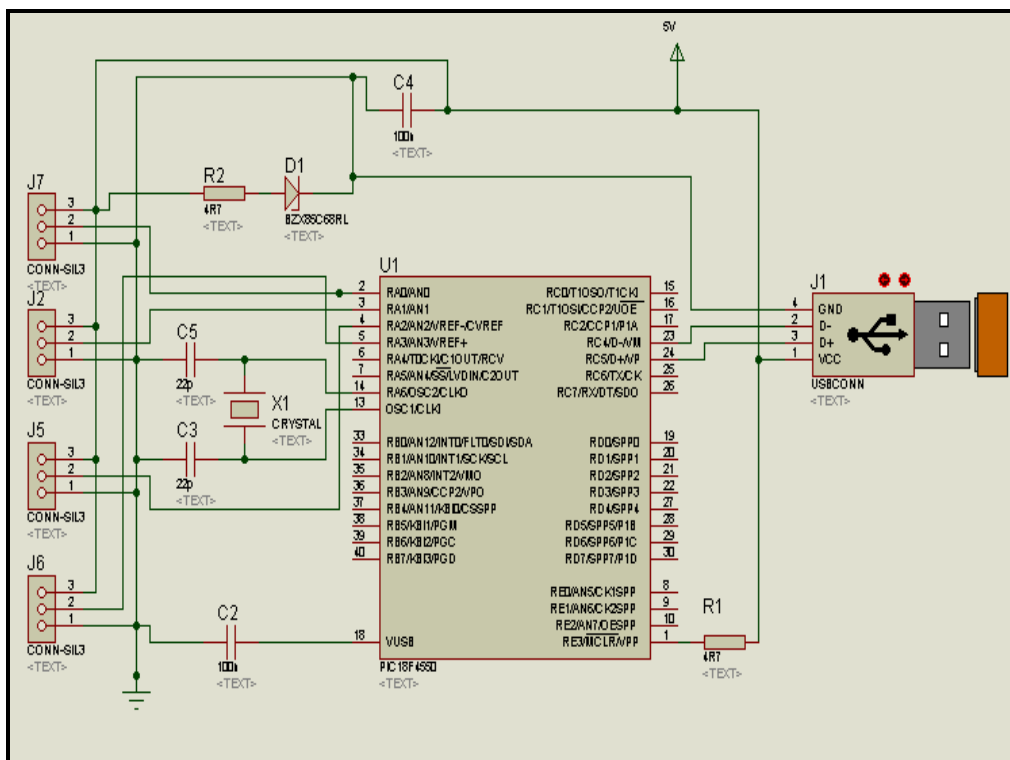


Fig.7. MCU board for acquiring sensor data for one joint

For the interaction module with human via the PC, we have chosen National Instruments® (NI) LabVIEW™ software [26, 27] to design the Human Machine Interfaces and to deploy and execute the customized control application on the hardware device. As shown in Fig.8, an intelligent Control Interface is proposed to help therapists to configure the robot and to tune the controller parameters. When the patient comes for a therapy, the therapist must load the patient’s information, adjust the robot parameters and tune the safe controller of the robot-aided therapy and then execute the controller application. Fig.9 shows the LabVIEW software design of the Controller Interface composed of two parts: in top, we can observe the code for the generation of the control law and, down, the case structure for the USB port configuration acquiring sensor data.

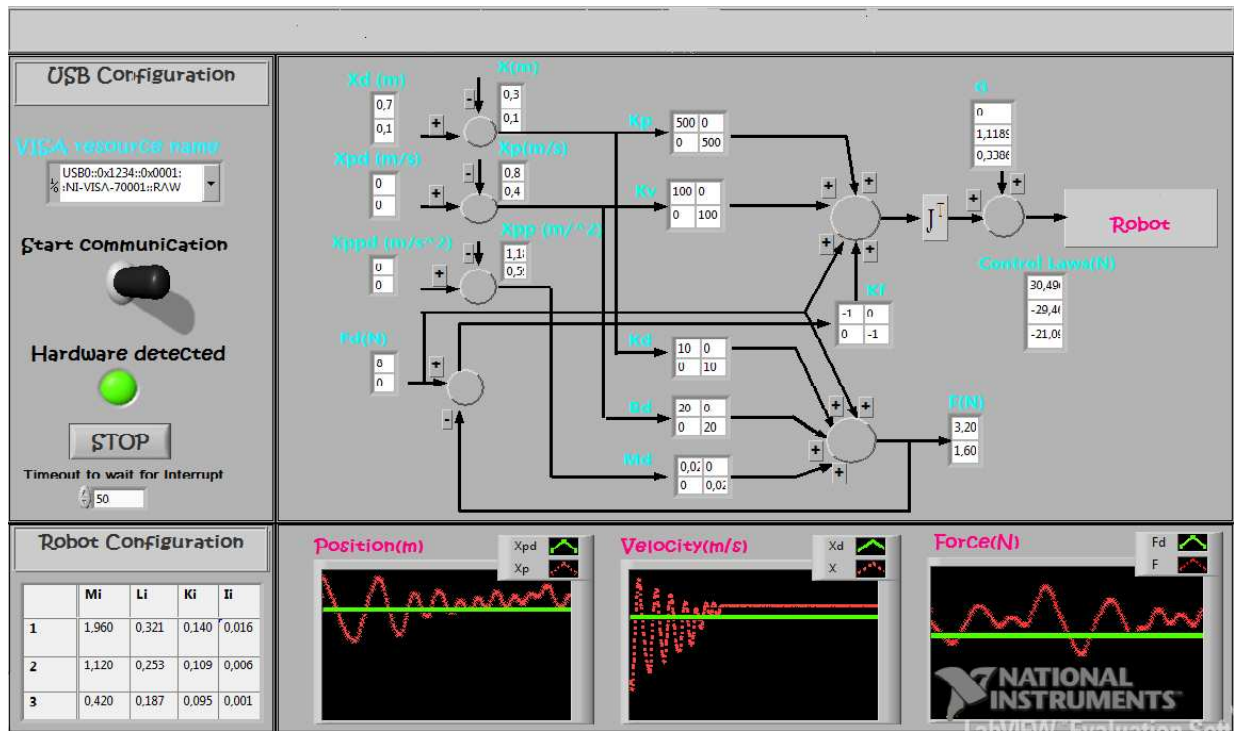


Fig.8. Controller Interface

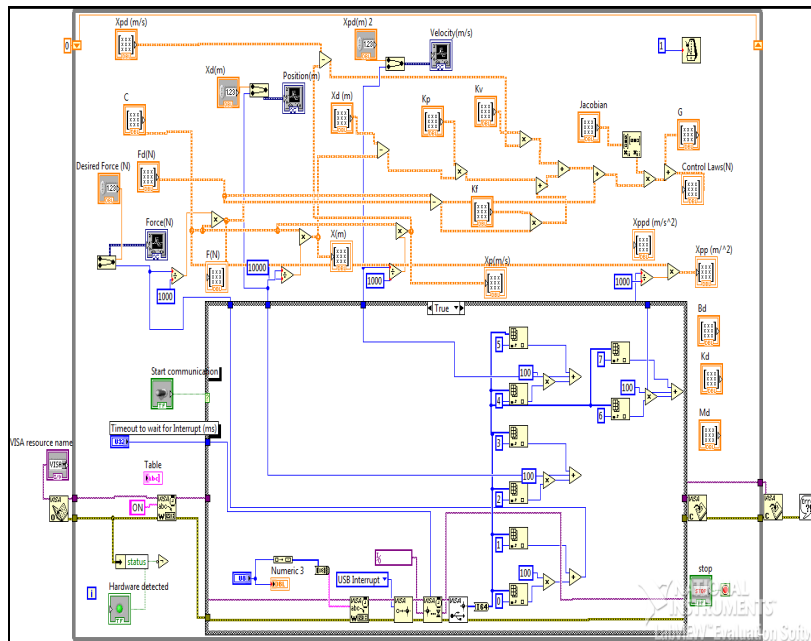


Fig.9. LabVIEW software design of the controller interface

Furthermore, we propose a Therapist-Patient Interface to motivate patient during the assessment treatment progress. Such interface should include the configuration of the training mode and must display training data (see Fig.10).

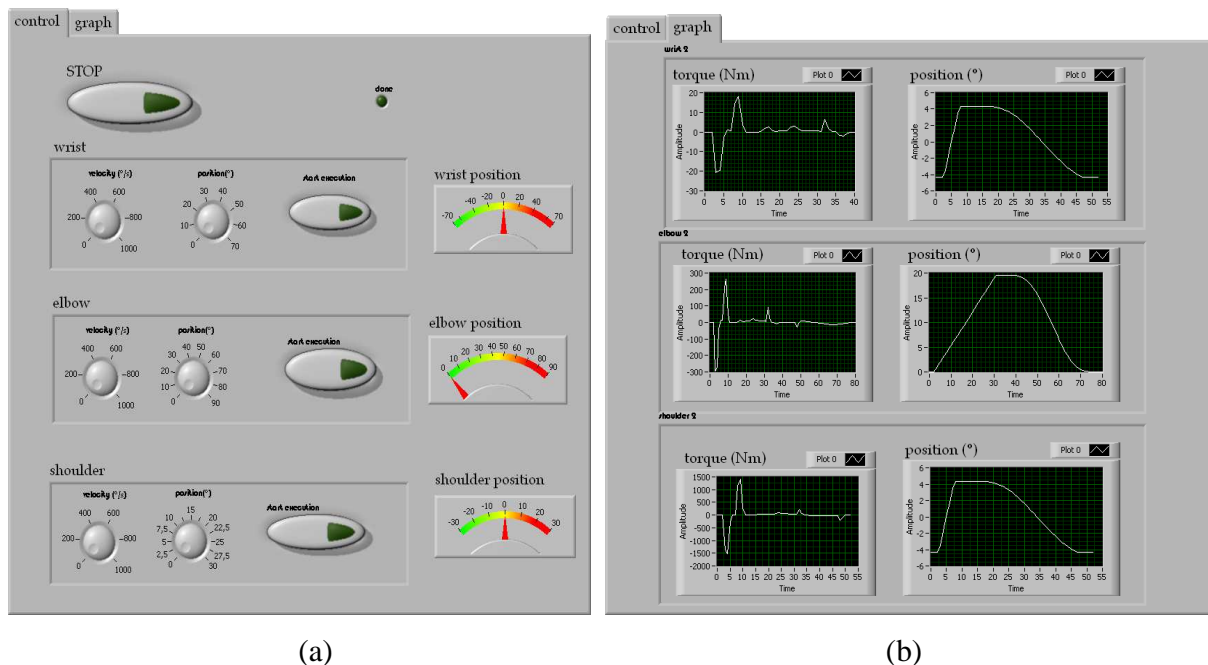


Fig.10. Therapist-Patient Interface: (a) training mode configuration (b) Graph display

VII. CONCLUSION

In this paper, design, control and optimization of a robot-assisted therapy are proposed. Human machine interfaces are also designed to help the therapist to tune the controller parameters based on the patient information and to motivate the patient during the assessment treatment progress. In this paper, safety was the main issue for the control design and optimization. However, we will consider in future works the compromise between robustness and safety criteria [28, 29]. Furthermore, to limit the vibrations of the assistive device, we will consider optimal trajectories with minimum jerk criteria [30, 31].

REFERENCES

- [1] M. Hillman, "Rehabilitation robotics from past to present - a historical perspective," *In Proc. 8th International Conference on rehabilitation Robotics (ICORR 2003)*, South Korea, 2003.
- [2] K. Kiguchi, S. Kariya, K. Watanabe, K. Izumi, T. Fukuda, "An exoskeletal robot for human elbow motion support—sensor fusion, adaptation, and control," *IEEE Transactions on Systems Man and Cybernetics, Part B*, vol. 31, n°3, 2001, pp. 353-361.
- [3] J.B. Stephen, E.B. Ian, H.S. Stephen, "Performance evaluation of a planar 3DOF robotic exoskeleton for motor assessment," *Journal of Medical Devices*, vol. 3, 2009, pp.1-12.
- [4] D.J. Reinkensmeyer, D. Aoyagi, J. L. Emken, J. A. Galvez, W. Ichinose, G. Kerdanyan, S. Maneekobkunwong, K. Minakata, J. A. Nessler, R. Weber, R. R. Roy, R. de Leon, J. E. Bobrow, S. J. Harkema, V. R. Edgerton, "Tools for understanding and optimizing robotic gait training," *Journal of Rehabilitation Research and Development*, vol. 43, 2007, pp.657-670.
- [5] J.F. Veneman, R. Kruidhof, E.E.G. Hekman, R. Ekkelenkamp, E.H.F.V. Asseldonk, H. V. D. Kooij, "Design and evaluation of the LOPES exoskeleton robot for interactive gait rehabilitation," *IEEE Transactions on Neural and Rehabilitation Systems Engineering*, vol. 15, n°3, 2007, pp. 379-386.
- [6] J.J. Daly, N. Hogan, E.M. Perepezko, et al., "Response to upper-limb robotics and functional neuromuscular stimulation following stroke," *Journal of Rehabilitation Research & Development*, vol. 42, n°6, 2005, pp. 723-736.

- [7] G. Romer, H. Stuyt, A. Peters, “Cost-savings and economic benefits due to the assistive robotic manipulator (ARM),” *In Proc. of the 9th international conference on rehabilitation robotics (ICORR 2005)*, Illinois (Chicago), 2005, pp. 201-204.
- [8] H. I. Krebs, J. J. Palazzolo, L. Dipietro, M. Ferraro, J. Krol, K. Ranekleiv, B. T. Volpe, N. Hogan, “Rehabilitation robotics: Performance-based progressive robot-assisted therapy,” *Autonomous Robots*, vol. 15, n°1, 2003, pp. 7-20.
- [9] P.S. Lum, C. G. Burgar, H.F.M. Van der Loos, P.C. Shor, M. Majmundar, R. Yap, “MIME robotic device for upper-limb neuro-rehabilitation in sub acute stroke subjects: A follow-up study,” *Journal of Rehabilitation Research & Development*, vol.43, n° 5, 2006, pp. 631-642.
- [10] T. G. Sugar, J.He, E.J. Koeneman, J.B. Koeneman, R.Herman, H. Huang, R.S. Schultz, D.E. Herring, J.Wanberg, S. Balasubramanian, P. Swenson, J.A. Ward, “Design and control of RUPERT: A device for robotic upper extremity repetitive therapy,” *IEEE Transactions on Neural Systems and Rehabilitation Engineering*, vol.15, n°3, 2007, pp. 336-346.
- [11] M. Yamano, Y. Suzukawa, J. Berengueres, R. Tadakuma, “Flexible control system of a robot hand using micro control units and RT-middleware,” *International Journal of Social Robotics*, DOI 10.1007/s12369-011-0130-y.
- [12] H. Mehdi, O. Boubaker, “Stiffness and impedance control using Lyapunov theory for robot-aided rehabilitation,” *International Journal of Social Robotics*, DOI: 10.1007/s12369-011-0128-5.
- [13] G. Herrmann & C. Melhuish, “Towards safety in human robot interaction,” *International Journal of Social Robotics*, vol. 2, n°3, 2010, pp. 217-219.
- [14] M. Vermeulen, M. Wisse, “Intrinsically safe robot arm: Adjustable static balancing and low power actuation,” *International Journal of Social Robotics*, vol. 2, n°3, 2010, pp. 275-288.
- [15] M. Van Damme, P. Beyl, B. Vanderborght, R. Versluys, R. Van Ham, I. Vanderniepen, F. Daerden, D. Lefeber, “The safety of a robot actuated by pneumatic muscles—A case study,” *International Journal of Social Robotics*, vol. 2, n°3, 2010, pp. 289-303.
- [16] S. M. M. Rahman and R. Ikeura, “Optimizing perceived heaviness and motion for lifting objects with a power assist robot system considering change in time constant,” *International Journal on Smart Sensing and Intelligent Systems*, vol.5, n°2, 2012, pp. 458-486.

- [17] N. Hogan, "Impedance control: An approach to manipulators: Part 1, 2, 3", *ASME Journal of Dynamic Systems, Measurement and Control*, vol. 107, n° 1, 1985, pp. 1-24.
- [18] H. Mehdi, O. Boubaker, "Rehabilitation of a human arm supported by a robotic manipulator: A position/force cooperative control," *Journal of Computer Science*, vol.6, n° 8, 2010, pp. 912-919.
- [19] H. Mehdi, O. Boubaker, "Impedance controller tuned by particle swarm optimization for robotic arms," *International Journal of Advanced Robotic Systems*, vol.8, n°5, 2011, pp.93-103.
- [20] H. Mehdi, O. Boubaker, "Position/force control optimized by particle swarm intelligence for constrained robotic manipulators," *In Proc. Of the 11th IEEE International Conference on Intelligent Systems Design and Applications (ISDA'2011)*, Córdoba, Spain, 2011, pp. 190-195.
- [21] A. Aloulou, O. Boubaker, "Control of a step walking combined to arms swinging for a three dimensional humanoid prototype," *Journal of Computer Science*, vol. 6, n° 8, 2010, pp. 886-895.
- [22] P.E. Gill, W. Murray, M.H. Wright, "Practical optimization," Academic Press, 1981.
- [23] M. P. Singh, P. K. Tripathi, K.V Gangadharan, "FPGA based vibration control of a mass varying two-degree of freedom system," *International Journal on Smart Sensing and Intelligent Systems*, vol.4, n°4, 2011, pp. 698-709.
- [24] W. Benrejeb, O. Boubaker, "FPGA modeling and real-time embedded control design via LabVIEW Software: Application for swinging-Up a pendulum," *International Journal on Smart Sensing and Intelligent Systems*, vol. 5, n°3, 2012, pp. 576-591.
- [25] K. Dhanalakshmi, Aditya Avinash, M. Umopathy, M. Marimuthu, "Experimental study on vibration control of shape memory alloy actuated flexible beam," *International Journal on Smart Sensing and Intelligent Systems*, vol. 3, n°2, 2010, pp. 156-175.
- [26] O. Boubaker, "National Instruments LabVIEW: Ultimate Software for Engineering Education," *in Proc. International Conference on Frontiers in Education: Computer Science and Computer Engineering*, Las Vegas, 2011.
<http://cerc.wvu.edu/download/WORLDCOMP%2711/2011%20CD%20papers/FEC4450.pdf>
- [27] The National Instruments® LabVIEW™ Corporation website (2010). [Online]. Available: <http://www.ni.com/labview/>

- [28] H. Mehdi, O. Boubaker, "Robust tracking control for constrained robots," *Procedia Engineering*, vol. 41, 2012, pp. 1292-1297.
- [29] H. Mehdi, O. Boubaker, "New robust tracking control for safe constrained robots under unknown impedance environment," *Lecture Notes in Computer Science*, vol. 7429, 2012, pp. 313-323.
- [30] A. Aloulou, O. Boubaker, "Minimum jerk-based control for a three dimensional bipedal robot," *Lecture Notes in Computer Science*, vol. 7102, 2011, pp. 251-262.
- [31] F. Kunwar, B. Benhabib, "Advanced predictive guidance navigation for Mobile Robots: A novel strategy for rendezvous in dynamic settings," *International Journal on Smart Sensing and Intelligent Systems*, vol. 1, n°4, 2008, pp. 858-890.